

STUDY OF THE INCLUSIVE REACTION $\gamma p \rightarrow \pi^- + \text{ANYTHING}$
IN THE PROTON FRAGMENTATION REGION*

W. P. Swanson, M. Davier, I. Derado[†], D. C. Fries^{††}, F. F. Liu^{†††},
R. F. Mozley, A. C. Odian, J. Park, F. Villa and D. E. Yount^{††††}

Stanford Linear Accelerator Center
Stanford University, Stanford, California 94305

ABSTRACT

The inclusive reaction $\gamma p \rightarrow \pi^- + \text{anything}$ is studied in the energy range $E_\gamma = 5.5 - 15$ GeV using the SLAC 2-meter streamer chamber. Experimental data on the differential cross section $\partial^2\sigma/\partial P_L \partial P_T^2$ in the target fragmentation region are qualitatively similar in shape but the magnitude shows a significant decrease with E_γ in this energy range.

(Submitted to Phys. Rev. Letters.)

* Work supported by the U. S. Atomic Energy Commission.

[†]Max-Planck-Institut für Physik und Astrophysik, Munich, Germany.

^{††}Institut für Experimentale Kernphysik, Universität Karlsruhe, Germany.

^{†††}Physics Department, CSC-San Bernardino, California.

^{††††}Department of Physics and Astronomy, University of Hawaii, Honolulu, Hawaii.

The term "inclusive reaction" has been used by Feynman to designate a class of reactions in which a particular type of particle (e.g., π^-) is detected in the final state, disregarding all other particles.¹ The variables which describe an inclusive reaction are P_T , x , and s , where P_T is the transverse momentum, s is the total c.m. energy squared, and $x \equiv 2 P_L^*/\sqrt{s}$, where P_L^* is the c.m. longitudinal momentum. Guided by general observations on the structure of field theory, Feynman hypothesized that at sufficiently high energy, the distribution of particles in an inclusive reaction should become a function of P_T and x only. This is the scaling hypothesis. Yang and coworkers² have emphasized a related concept called limiting fragmentation. In this scheme, the distribution of particles of a given type is studied in the target (or projectile) rest system. This distribution $\rho(P_L, P_T)$ should approach a limit as the projectile energy increases. It can be shown that these two hypotheses are equivalent at high energies.³

Experimentally, the hypothesis of limiting fragmentation is approximately true for $pp \rightarrow \pi^\pm + \text{anything}$ in the range 12 - 70 GeV/c,⁴ for $\pi^- p \rightarrow \pi^\pm + \text{anything}$ in the range 2.5 - 25 GeV/c,⁵ and $K^+ p \rightarrow \pi^- + \text{anything}$ at 12 GeV/c⁶ at least in the target fragmentation region. Thus it would be a very intriguing observation if the same were true for photon-induced reactions. It is well known that γp reactions have many features in common with $\pi^\pm p$ interactions. The total cross sections have a very similar energy behavior (scaled by about a factor of 200), the average transverse momentum is small ($\langle P_T \rangle \sim 0.3$ GeV/c) in both cases, and many of the same resonances are observed. These observations are approximately explained by the notion of vector-dominance: The hadron-like properties of the photon apparently arise because it has the same quantum numbers as the vector mesons (ρ, ϕ, ω). Thus limiting fragmentation may also be a property that γp has in common with πp , pp and perhaps with other hadron-hadron collisions.

We present here results for $\gamma p \rightarrow \pi^- + \text{anything}$. Multiparticle final states have been studied using the SLAC 2-meter streamer chamber.⁷ Important features of the experiment are the 18-GeV Bremsstrahlung beam, the pressurized hydrogen target, the 10.4 kG magnetic field, and 600,000 stereoscopic triads. The events studied in this analysis are the 3, 5, 7 and 9-prong topologies (21055, 15304, 1918, and 184 events, respectively). These numbers of events correspond to different film samples, and appropriate weights were therefore used for each topology.

We adopt the Yang approach in examining distributions of negative tracks in the target rest system (laboratory). This approach is the most direct and simple application of our data, and it also allows easy comparison with other experiments.⁸

An experimental complication arises from the fact that the photon beam contains all energies up to 18 GeV, and therefore the energy of a given event is not exactly determinable if neutral particles are emitted. Nevertheless, we test the hypothesis of limiting fragmentation in the target-fragmentation region in the following way: We first calculate the "visible" laboratory photon energy $E_{\text{vis}} \equiv |\sum \vec{P}_i|$ for each event. The index i refers to the charged tracks. Note that $E_{\text{vis}} \leq E_\gamma$, where E_γ is the true laboratory energy. We then choose particular energy intervals in E_{vis} and assign each event to the appropriate interval. In general, events with neutrals that carry off a small amount of energy will fall in the proper interval, while those having a large amount of energy taken by the neutrals will fall in a lower E_{vis} interval. This may introduce some distortion into the distributions of low-energy pions examined. However, it would seem unlikely that distributions which vary in shape with E_γ would be distorted in such a way as to show shapes independent of E_{vis} , because the low-energy particles studied make relatively little contribution to E_{vis} . At least on the basis of

energy-balance considerations the E_{vis} assignment is relatively insensitive to the configuration of the target fragmentation particles. Thus if the data, treated in this manner, show apparent limiting in the shapes of the distributions, this can be taken as evidence for approximate actual limiting in shape.

We test for limiting in magnitude as well as shape, combining the data by means of the formula

$$\frac{\partial^2 \sigma(E_{\text{vis}})}{\partial P_L \partial P_T^2} \equiv \frac{\partial^2 \sigma(E_\gamma; \pm)}{\partial P_L \partial P_T^2} + \left[\frac{\sigma_{\text{tot}}(E_\gamma) - \sigma(E_\gamma; \pm)}{\sigma(E_{\text{vis}}; \pm 0)} \right] \frac{\partial^2 \sigma(E_{\text{vis}}; \pm 0)}{\partial P_L \partial P_T^2} \quad (1)$$

The first term is based on the subsample of events containing only charged particles in the final state (designated \pm) and having energy E_γ that is therefore known. The second term is based on the subsample of events having at least one neutral (± 0) which are therefore classified according to E_{vis} . The apparent differential cross section $\partial^2 \sigma(E_{\text{vis}}; \pm 0) / \partial P_L \partial P_T^2$ is multiplied by a factor which is intended to correct for the loss of events from higher-energy intervals to lower-energy ones, owing to the use of E_{vis} rather than E_γ . Values of $\sigma_{\text{tot}}(E_\gamma)$ are taken from a UCSB-SLAC collaboration,⁹ whereas $\sigma(E_\gamma; \pm)$ and $\sigma(E_{\text{vis}}; \pm 0)$ are derived from the present experiment. The data, corrected in this way, are presented in Figs. 1 and 2. The accuracy of this correction is discussed below.

In Fig. 1, we compare the shape of the P_T^2 distribution for four E_{vis} intervals ranging from 5.5 - 15 GeV. All negative tracks from all topologies are combined, using a weighting based on the differing film samples used and on the event geometrical configuration.¹⁰ Based on the number of K^\pm particles present in 3-constraint events, we estimate that about 95% of the negative tracks are π^- . In Fig. 1, the experimental differential cross section $\partial^2 \sigma(E_{\text{vis}}) / \partial P_L \partial P_T^2$ is integrated over an interval in P_L ($-0.3 < P_L < 0.3$ GeV/c) near zero in the

laboratory system. Only representative error bars are shown. There is qualitative similarity in shape although the higher E_{vis} points appear to decrease with P_{T}^2 at a somewhat faster rate.

Figure 2 shows distributions of P_{L} (Lab) for a particular P_{T} interval ($0.1 < P_{\text{T}} < 0.2$ GeV/c). This restricted P_{T} range is near the maximum in P_{T} and is chosen in order that the connection between P_{L} and x may be approximately calculated. This distribution remains qualitatively similar over the E_{vis} range studied, but we note an apparent trend in that the cross sections decrease somewhat with E_{vis} .

We have used various models to understand the comparison in E_{vis} and its relationship to a comparison in E_{γ} . An increment in E_{vis} contains two contributions corresponding to the two terms of Eq. (1): (1) events with no neutral particles, and (2) a contribution of events of higher energy E_{γ} where a fraction of the energy is carried off by neutral particles:

$$\frac{\partial^2 \sigma(E_{\text{vis}})}{\partial P_{\text{L}} \partial P_{\text{T}}^2} = \frac{\partial^2 \sigma(E_{\gamma}; \pm)}{\partial P_{\text{L}} \partial P_{\text{T}}^2} + \int_{E_{\text{vis}}}^{18 \text{ GeV}} \frac{\partial^2 \sigma(E'_{\gamma}; \pm 0)}{\partial P_{\text{L}} \partial P_{\text{T}}^2} Q(E'_{\gamma}, E_{\text{vis}}) \frac{dE'_{\gamma}}{E'_{\gamma}} + \sigma(E_{\gamma}; \pm 0) \cdot \frac{\int_{E_{\text{vis}}}^{18 \text{ GeV}} \sigma(E'_{\gamma}; \pm 0) Q(E'_{\gamma}, E_{\text{vis}}) \frac{dE'_{\gamma}}{E'_{\gamma}}}{\int_{E_{\text{vis}}}^{18 \text{ GeV}} \sigma(E'_{\gamma}; \pm 0) Q(E'_{\gamma}, E_{\text{vis}}) \frac{dE'_{\gamma}}{E'_{\gamma}}} \quad (2)$$

where $Q(E_{\gamma}, E_{\text{vis}}) dE_{\text{vis}}$ is the probability that an event of energy E_{γ} has a visible energy between E_{vis} and $E_{\text{vis}} + dE_{\text{vis}}$. In this formulation, we assume that $Q(E_{\gamma}, E_{\text{vis}})$ does not depend on \vec{P} of the low-energy π^- under consideration, as these particles do not affect the energy balance significantly. This assumption is consistent with the approximately constant shape which we see in Figs. 1 and 2.

To obtain concrete results, we have assumed¹¹ various behaviors for $Q(E_\gamma, E_{\text{vis}})$ and have computed Eq. (2). We have found that an E_{vis} dependence of the amount seen in Fig. 2 is caused by an even stronger E_γ dependence. The relationship between the experimental $\partial^2\sigma(E_{\text{vis}})/\partial P_L \partial P_T^2$ as calculated from the data using Eq. (1), and the corresponding inclusive cross section $\partial^2\sigma(E_\gamma)/\partial P_L \partial P_T^2$ at a given E_γ was numerically determined from these computations. The required correction is less than 10% everywhere, and is relatively independent of the form of $Q(E_\gamma, E_{\text{vis}})$.

In order to gain sufficient statistics to study the trend seen in Fig. 2, we have integrated $\partial^2\sigma(E_\gamma)/\partial P_L \partial P_T^2$ over all P_T^2 and over the range $-\infty < P_L < 0.0$ GeV/c for each E_γ interval:

$$S_{-\infty}^{0.0}(E_\gamma) \equiv \int_{-\infty}^{0.0 \text{ GeV/c}} \int_0^\infty \frac{\partial^2\sigma(E_\gamma)}{\partial P_L \partial P_T^2} dP_T^2 dP_L$$

This region of backward π^- is presumably richer in proton fragmentation than the entire P_L range shown in Fig. 2.

After all corrections have been made, we find the values $S_{-\infty}^{0.0}(E_\gamma) = 3.78 \pm 0.44$, 3.83 ± 0.34 , 3.10 ± 0.32 and 2.47 ± 0.32 μb , for E_γ intervals centered at 5.5, 7.5, 10.5 and 15 GeV, respectively. The individual errors reflect statistics, uncertainties in the parameters of Eq. (1), and an uncertainty in the translation from E_{vis} to E_γ . In addition, we estimate an overall normalization uncertainty of ± 0.3 μb , owing to the simplifications inherent in Eq. (2).

At these energies, the regions of target and beam fragmentation may overlap appreciably. Thus, even the backward region considered may contain a π^- contribution from other than proton fragmentation, and an interpretation of the observed decrease of the π^- yield with E_γ may be difficult. Nevertheless,

assuming that the region is dominated by proton fragmentation, it is interesting to parameterize the yields $S_{-\infty}^{0.0}$ in a form suggested by Regge phenomenology for target fragmentation¹²: $S_{-\infty}^{0.0} = A + B s^{-1/2}$. A least-squares fit yields $A = (0.1 \pm 1.1) \mu\text{b}$ and $B = (13.4 \pm 4.4) \mu\text{b GeV}$.¹³ Thus, assuming this parameterization to be valid, it would seem that the cross section in the target-fragmentation region in the E_{γ} range studied is significantly above its asymptotic value.

We gratefully acknowledge the efforts of Leroy Schwarcz, our engineers, technicians, programmers and scanners. We are indebted to James Bjorken, Clifford Risk and Christopher Quigg for stimulating theoretical discussions.

REFERENCES

1. R. P. Feynman, in Proceedings of the Third International Conference -- High Energy Collisions, Stony Brook, 1969, edited by C. N. Yang *et al.*, (Gordon and Breach, New York, 1969); Phys. Rev. Letters 23, 1415 (1969).
2. J. Benecke, T. T. Chou, C. N. Yang, and E. Yen, Phys. Rev. 188, 2159 (1969); T. T. Chou and C. N. Yang, Phys. Rev. Letters 25, 1072 (1970).
3. J. C. Van der Velde, Phys. Rev. Letters 32B, 501 (1970).
4. (a) D. B. Smith, R. J. Sprafka and J. A. Anderson, Phys. Rev. Letters 23, 1064 (1969); (b) S. D. Drell, SLAC-PUB-745 (May, 1970); (c) Dennis B. Smith, Ph.D. Thesis, UCRL-20632 (March, 1971); (d) J. C. Van der Velde, Phys. Rev. Letters 32B, 501 (1970); (e) H. Boggild, K. H. Hansen and M. Suk, Nucl. Phys. B27, 1 (1971).
5. (a) Min-Shih Chen, Ling-Lie Wang and T. F. Wong, Phys. Rev. Letters 26, 280 (1971); (b) R. W. Anthony, C. T. Coffin, E. S. Meanley, J. E. Rice, K. M. Terwilliger, and N. R. Stanton, Phys. Rev. Letters 26, 38 (1971); (c) H. Piotrowska, Phys. Letters 32B, 71 (1970).
6. W. Ko and R. L. Lander, Phys. Rev. Letters 26, 1064 (1971). In this paper a comparison is made of the x-distribution of π^- in $K^+p \rightarrow \pi^-$ and $\pi^-p \rightarrow \pi^-$.
7. The experimental arrangement is similar to that described in: M. Davier, I. Derado, D. Drickey, D. Fries, R. Mozley, A. Odian, F. Villa and D. Yount, Phys. Rev. D1, 790 (1970).
8. Such comparisons have been made between: (a) $K^+p \rightarrow \pi^-$ (12 GeV/c) and $\pi^-p \rightarrow \pi^-$ (25 GeV/c): W. Ko and R. L. Lander, Phys. Rev. Letters 26, 1064 (1971); (b) $\pi^+p \rightarrow \pi^-$ (7 GeV/c), $K^+p \rightarrow \pi^-$ (12.7 GeV/c), $pp \rightarrow \pi^-$ (28.5 GeV/c), $\pi^-p \rightarrow \pi^-$ (24.8 GeV/c), $\pi^-p \rightarrow \pi^+$ (24.8 GeV/c); M.-S. Chen, R. R. Kinsey,

- T. W. Morris, R. S. Panvini, L.-L. Wang, T. F. Wong, S. L. Stone, T. Ferbel, P. Slattery, B. Werner, J. W. Elbert and A. R. Erwin, Phys. Rev. Letters 26, 1585 (1971); (c) $\pi^+p \rightarrow \pi^-$ (18.5 GeV/c), $\pi^-p \rightarrow \pi^-$ (18.5 GeV/c), $pp \rightarrow \pi^-$ (18.5 GeV/c): N. N. Biswas, N. M. Cason, V. P. Kenney, J. T. Powers, W. D. Shephard and D. W. Thomas, Phys. Rev. Letters 26, 1589 (1971); (d) $pp \rightarrow \pi^-$ (28.5 GeV/c), $K^+p \rightarrow \pi^-$ (11.8 GeV/c), $\gamma p \rightarrow \pi^-$ (6-18 GeV, this experiment): W. P. Swanson, W. Ko, R. L. Lander, C. Risk, R. R. Ross and D. B. Smith, SLAC-UC Davis-LRL collaboration, in preparation.
9. D. O. Caldwell, V. B. Elings, W. P. Hesse, R. J. Morrison, F. V. Murphy, B. W. Worster and D. E. Yount, Phys. Rev. Letters 25, 609 (1970).
 10. SLAC Technical Note, Group D, in preparation.
 11. The various forms for the E_{vis} dependence of $Q(E_\gamma, E_{\text{vis}})$ included: (a) a linear rise from zero at $E_{\text{vis}}=0$; (b) a linear fall to zero at $E_{\text{vis}}=E_\gamma$; (c) a parabolic behavior, and (d) constant. The behaviors (a) and (b), which we consider extremes, were used as a basis for obtaining the uncertainty in the correction from E_{vis} to E_γ .
 12. See, for example, Chan Hong-Mo, C. S. Hsu, C. Quigg and Jiuun-Ming Wang, Phys. Rev. Letters 26, 672 (1971).
 13. If we integrate over the larger range $-\infty < P_L < 0.5$ GeV/c, adopted by a BNL-Rochester-Wisconsin collaboration (Ref. 8b), we find $S_{-\infty}^{0.5}(E_\gamma) = 52.4 \pm 2.8, 47.5 \pm 2.3, 44.4 \pm 1.9,$ and $38.8 \pm 1.6 \mu\text{b}$ for E_γ intervals centered at 5.5, 7.5, 10.5, and 15 GeV, respectively, with an overall normalization uncertainty of $\pm 5 \mu\text{b}$. A least-squares fit, similar to that described in the text, yields $A = (16 \pm 6) \mu\text{b}$ and $B = (124 \pm 26) \mu\text{b GeV}$ when applied to these results. An overall normalization uncertainty of $\pm 5 \mu\text{b}$ is not included in the errors quoted.

14. A similar study has been made at photon energies $E_\gamma = 2.8, 4.7$ and 9.3 GeV by the SLAC-Berkeley-Tufts collaboration: J. Ballam, G. B. Chadwick, M. Della-Negra, R. Gearhart, K. C. Moffeit, J. J. Murray, P. Seyboth, C. K. Sinclair, I. O. Skillicorn, H. Spitzer, G. Wolf, H. H. Bingham, W. B. Fretter, W. J. Podolsky, M. S. Rabin, A. H. Rosenfeld and R. Windmolders, contribution to the International Symposium on Electron and Photon Interactions at High Energies, Ithaca, N. Y., 1971, and private communication.

FIGURE CAPTIONS

1. Differential cross sections for the inclusive reaction $\gamma p \rightarrow \pi^- + \text{anything}$ for four intervals in E_{vis} . The error bars represent statistical errors only. We define "σ" to be the integral of $\partial^2 \sigma(E_{\text{vis}}) / \partial P_L \partial P_T^2$ between $P_L = -0.3$ and 0.3 GeV/c.
2. The differential cross section $\partial^2 \sigma(E_{\text{vis}}) / \partial P_L \partial P_T$ for $0.1 \leq P_T \leq 0.2$ GeV/c as a function of P_L . The error bars represent statistical errors only. The upper scale is x , evaluated for $P_T = 0.15$ GeV/c and representative photon energies $E_\gamma = 5.5$ and 15 GeV.

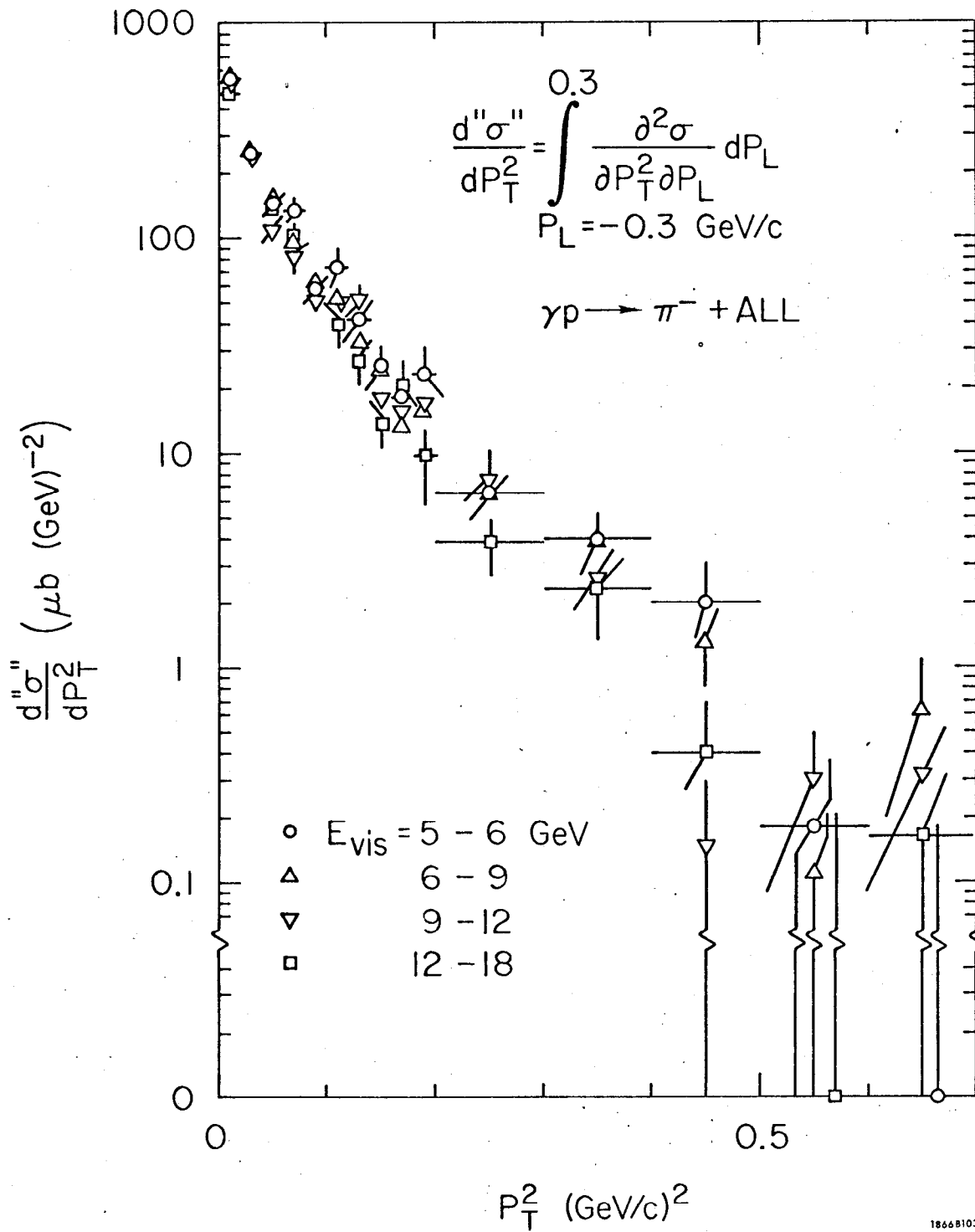


Fig. 1

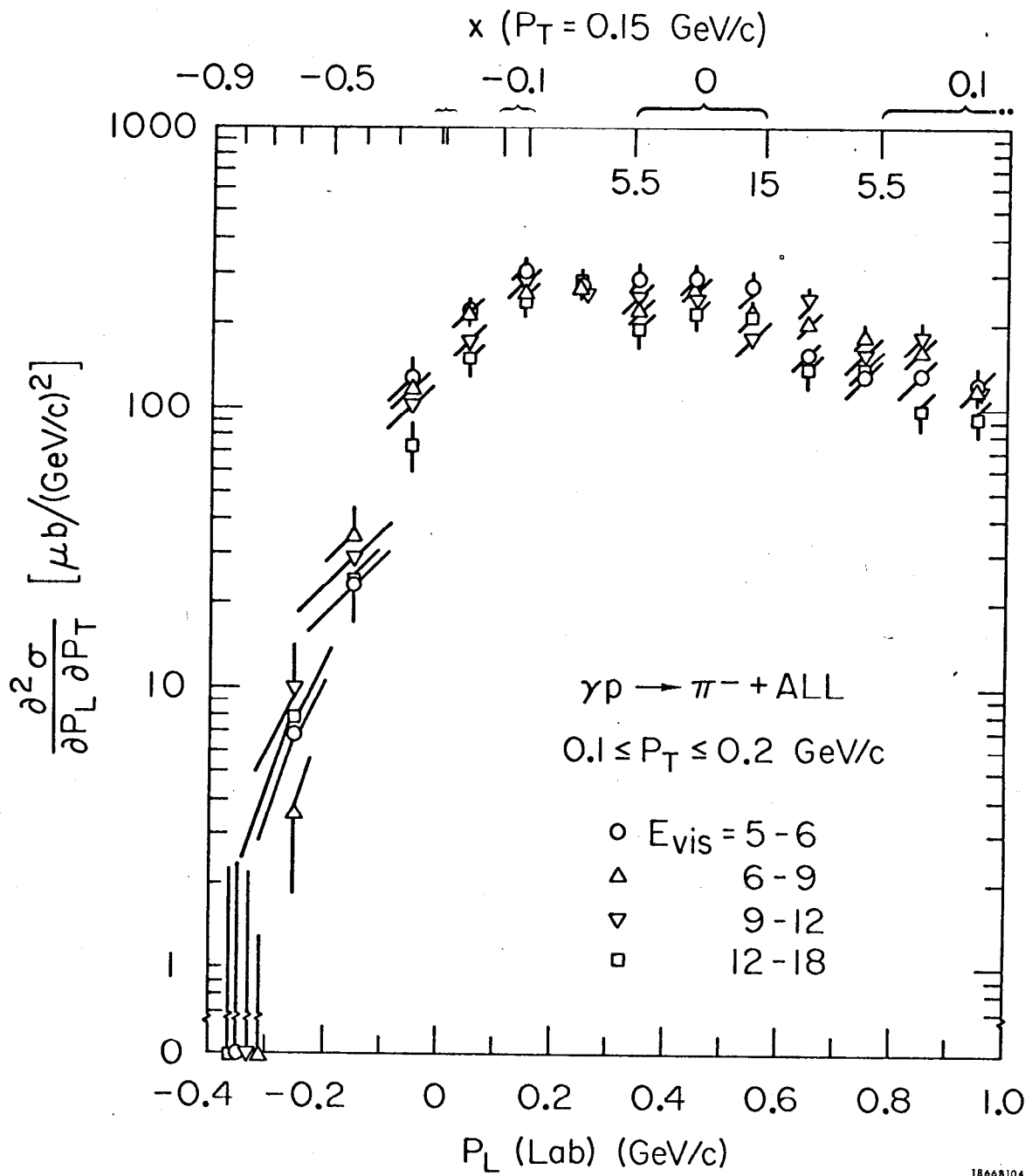


Fig. 2.